

Using Strain for the Reduction of Surface Roughness Induced Spin Relaxation in Field-Effect Transistors with Thin Silicon Body

Dmitri Osintsev, Viktor Sverdlov, and Siegfried Selberherr

Institute for Microelectronics, TU Wien, Gußhausstraße 27-29, A-1040 Wien, Austria
{osintsev|sverdlov|selberherr}@iue.tuwien.ac.at

1. Introduction

Utilizing spin properties of electrons opens great opportunities to reduce device power consumption in future electron devices. The spin of an electron can change its orientation to opposite very quickly by using an amazingly small amount of energy. Silicon, the main element of microelectronics, possesses several properties attractive for spin-driven applications: It is composed of nuclei with predominantly zero spin and it is characterized by small spin-orbit coupling. Spin transport through a 350µm thick silicon wafer was demonstrated [1]. Spin propagation at such long distances combined with a possibility of injecting spin at room temperature [2] makes the fabrication of spin-based switching devices in the near future quite plausible. However, the experimentally observed enhancement in spin relaxation in electrically gated lateral-channel silicon structures [3] could become an obstacle in realizing spin-driven devices, and a deeper understanding of fundamental spin relaxation mechanisms in silicon is urgently needed.

2. Method and Results

We investigate the surface roughness induced spin relaxation in a double-gate silicon spin field-effect transistors. To accurately describe the band structure in silicon in the presence of the intrinsic spin-orbit interaction we generalize the perturbative two-band $\mathbf{k}\cdot\mathbf{p}$ approach [4] to include the spin degree of freedom, similar to the recent work [5]. The Hamiltonian (1) (shown in Fig.1) is written in the vicinity of the X point along the k_z axis in the Brillouin zone. The basis is conveniently chosen as $[(X_1-X_2, \uparrow), (X_1-X_2, \downarrow), (X_1+X_2, \uparrow), (X_1+X_2, \downarrow)]$, where the up- and down-arrows indicate the spin projection at the quantization z -axis. Here m_t and m_l are the transversal and the longitudinal effective masses, $k_0 = 0.15 \times 2\pi/a$ is the position of the valley minimum relative to the X point in unstrained silicon, ε_{xy} denotes the shear strain component, $M^{-1} \approx m_t^{-1} - m_l^{-1}$, and $D=14\text{eV}$ is the shear strain deformation potential. The term proportional to

$$\Delta_x = 2 \sum \frac{\langle X_1 | p_x | n \rangle \langle n | \nabla V \times \mathbf{p} | X_2 \rangle}{E_n - E_x} \quad (2)$$

couples the states with the opposite spin projections. The two pairs of degenerate eigenvalues with opposite spin

projections, $|\uparrow\rangle$ and $|\downarrow\rangle$, correspond to the eigenvalues (3).

$$E = \frac{\hbar^2 k_z^2}{2m_l} + \frac{\hbar^2 (k_x^2 + k_y^2)}{2m_t} \pm \sqrt{\left(\frac{\hbar^2 k_z k_0}{m_l}\right)^2 + \left(D\varepsilon_{xy} - \frac{\hbar^2 k_x k_y}{M}\right)^2} + \Delta_x^2 (k_x^2 + k_y^2) \quad (3)$$

The degenerate states are chosen to satisfy $\langle \uparrow | \sigma_z | \downarrow \rangle = 0$. Each of these states is a linear combination of the states with up and down spin projection along the z -axis. The spin mixing is determined by the total magnitude of the spin-down projection which appears in the $|\uparrow\rangle$ state due to the spin-orbit interaction.

The surface roughness scattering between the subbands is taken to be proportional to the square of the product of the subband function derivatives at the interface [6]. A (001) silicon film of 5nm thickness is considered. The surface roughness at the two interfaces is assumed to be independent. It is described by a mean and a correlation length [4,6].

Shear strain makes the k_z band dispersion non-parabolic which leads to the energy splitting ΔE between the otherwise degenerate unprimed subbands [4]. This results in a slight strain dependence of the (normalized) intra-subband scattering rates between the states with the same spin projection (Fig.2). The inter-subband scattering rates at a fixed energy E decrease with shear strain. They become zero for $E < \Delta E$ (Fig.3).

Intra-subband spin relaxation rates decay rapidly with shear strain increased (Fig.4). The inter-subband spin relaxation appears to be a factor of two stronger due to the fact that spin coupling in (1) is between the states from the opposite valleys [5]. Inter-subband spin relaxation decreases with strain (Fig.5). Thus, applying uniaxial in-plane stress suppresses spin relaxation. Stress can be used to boost both mobility and spin lifetime.

References

- [1] B.Huang *et al.* *Phys. Rev. Lett.* **99**, 177209 (2007).
- [2] C.H.Li *et al.*, *Nature Comms* **2**, 245 (2011).
- [3] L.Li, I.Appelbaum, *Phys Rev.B.* **84**, 165318 (2011).
- [4]. V.Sverdlov. *Strain-Induced Effects in Advanced MOSFETs.*, Springer 2011.
- [5] P.Li, H.Dery, *Phys. Rev. Lett.* **107**, 107203 (2011).
- [6] M.Fischetti *et al.* *J.Appl.Phys.* **94**, 1079 (2003).

$$H = \begin{bmatrix} \frac{k_z^2}{2m_l} + \frac{k_0 k_z}{m_l} + \frac{k_x^2 + k_y^2}{2m_t} + U(z) & 0 & D\varepsilon_{xy} - \frac{k_x k_y}{M} & (k_y - k_x i)\Delta_{SO} \\ 0 & \frac{k_z^2}{2m_l} + \frac{k_0 k_z}{m_l} + \frac{k_x^2 + k_y^2}{2m_t} + U(z) & (-k_y - k_x i)\Delta_{SO} & D\varepsilon_{xy} - \frac{k_x k_y}{M} \\ D\varepsilon_{xy} - \frac{k_x k_y}{M} & (-k_y + k_x i)\Delta_{SO} & \frac{k_z^2}{2m_l} - \frac{k_0 k_z}{m_l} + \frac{k_x^2 + k_y^2}{2m_t} + U(z) & 0 \\ (k_y + k_x i)\Delta_{SO} & D\varepsilon_{xy} - \frac{k_x k_y}{M} & 0 & \frac{k_z^2}{2m_l} - \frac{k_0 k_z}{m_l} + \frac{k_x^2 + k_y^2}{2m_t} + U(z) \end{bmatrix} \quad (1)$$

Fig.1: Hamiltonian including strain obtained with the perturbative two-band $\mathbf{k}\cdot\mathbf{p}$ approach.

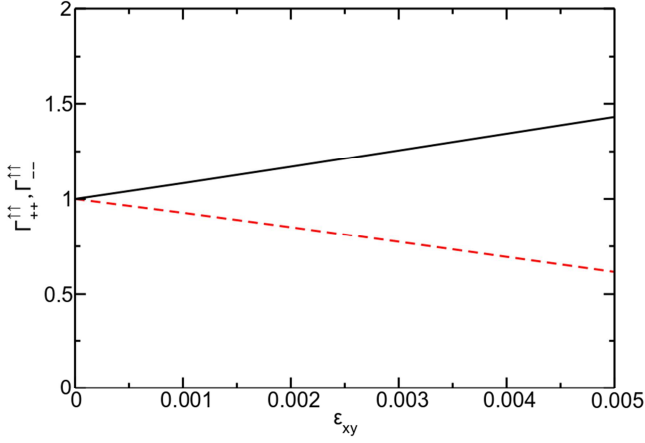


Fig.2: Intra-subband scattering rates between the states with the same spin projection.

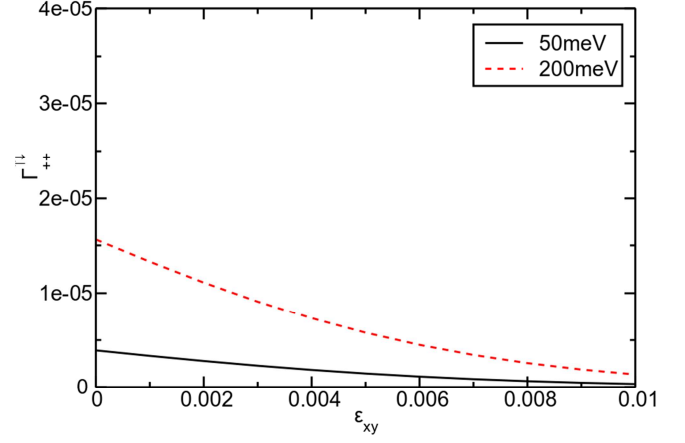


Fig.4: Intra-subband spin relaxation rate.

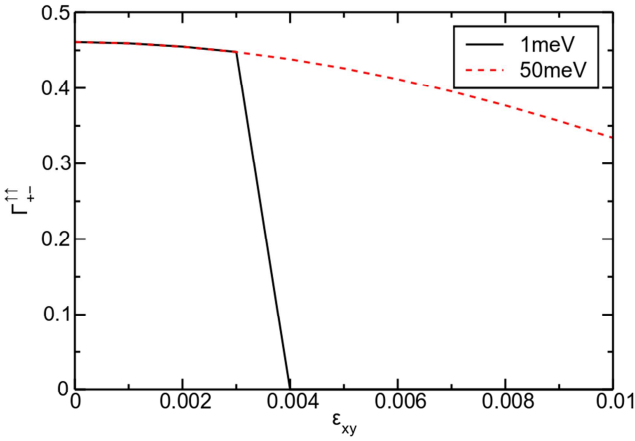


Fig.3: Inter-subband scattering between the states with the same spin projection.

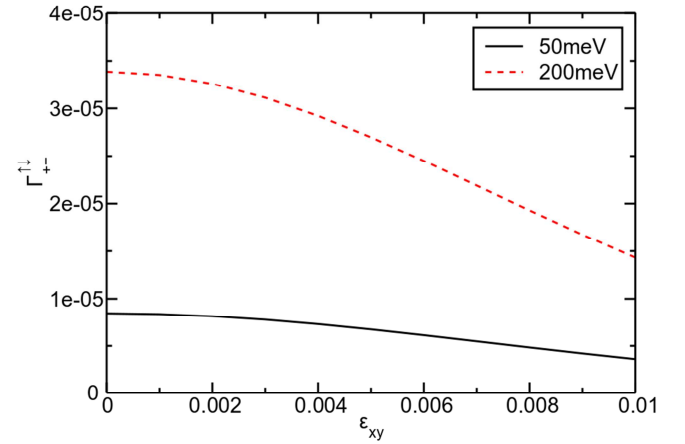


Fig.5: Inter-subband spin relaxation rate.

This work is supported by the European Research Council through the grant #247056 MOSILSPIN.